

Spectroscopic structure of two interacting electrons in a quantum dot by the shifted $1/N$ expansion method

Mohammad El-Said

Department of Physics, EMU, Gazi Magusa Mersin 10, Turkey

(Received 25 January 1999; revised manuscript received 27 January 2000)

The shifted $1/N$ expansion method has been used to study the relative Hamiltonian of two interacting electrons confined in a quantum dot. The eigenenergy spectra are obtained for any arbitrary ratio of Coulomb to confinement energies. Interesting features of the quantum dot spectra, such as the energy-level crossings and the removal of the degeneracy, are explained. Comparisons show that our results are in very good agreement with recent published ones calculated by exact and WKB methods.

I. INTRODUCTION

Quasi-zero-dimensional systems, such as quantum dots (QD's), have been the subject of intense research in recent years, owing to the nanofabrication techniques that make possible the realization of systems of very small dimensions comparable to the de Broglie wavelength of carriers. In such small structures the electrons are fully quantized into a discrete spectrum of energy levels. Different experimental¹⁻¹¹ and theoretical¹²⁻²⁶ methods have been devoted to investigate the energy spectrum and correlation effects of the interacting electrons confined in quantum dots under the effect of applied magnetic field. One of the most interesting features of the electrons confined in a quantum dot is the energy-level crossings. Once the crossings occur the spin and angular momentum quantum numbers of the ground state of the quantum dot changes. These spin transitions appear as a kink in the addition energy spectra of the electrons confined in a quantum dot. Indeed these kinks have also been experimentally confirmed in the addition energy $\mu(N_e)$ spectra of the quantum dot using the single-electron spectroscopy⁶ and gated transport spectroscopy methods.¹¹ The addition energy level $\mu(N_e)$, as usual, is the energy required to add one more electron to the QD, raising it from an $(N_e - 1)$ -electron ground state to an (N_e) -electron ground state; $\mu(N_e) = E_G(N_e) - E_G(N_e - 1)$.

In this work we shall use the $1/N$ expansion method to focus on the quantum dot confining two interacting electrons as a simple, but not trivial case. First we calculate the spectra of two interacting electrons confined in a parabolic quantum dot and, second, we give physical analysis to the crossing phenomena, which occur in the quantum dot spectra. We then compare our computed QD spectra in addition to the spin singlet-triplet transition with different theoretical works²¹ and relate our results with experimental^{6,7,10,11} works. The shifted $1/N$ expansion method has an advantage over methods such as perturbations and pure numerical calculations. While the $1/N$ expansion technique is valid for all the ranges of λ , the perturbation theory is limited to a weak range of λ only. Purely numerical calculations are computationally intensive and hard to follow in the physics of the problem.

The rest of this work is outlined as follows. In Sec. II, we

have presented the Hamiltonian theory for two interacting electrons parabolically confined in a quantum dot. We describe in Sec. III the shifted $1/N$ expansion technique, and the final section is devoted to results and conclusions.

II. THE HAMILTONIAN THEORY

The effective-mass Hamiltonian for two interacting electrons, confined by a harmonic potential of characteristic length $l_0 = (\hbar/m^* \omega_0)^{1/2}$ in the xy plane, can be decoupled to center-of-mass and relative motion as follows:

$$H_R = \frac{\mathbf{P}^2}{2M} + \frac{1}{2} M \omega_0^2 R^2, \quad (1)$$

$$H_r = \frac{P^2}{2\mu} + \frac{1}{2} \mu \omega_0^2 r^2 + \frac{e^2}{\epsilon |r|}. \quad (2)$$

For the center of mass $M = 2m^*$, $Q = 2e$, $\mathbf{P} = \mathbf{p}_1 + \mathbf{p}_2$ and its coordinate $\mathbf{r}_{cm} = (\mathbf{r}_1 + \mathbf{r}_2)/2$. Similarly, for the relative part we have reduced mass $\mu = m^*/2$, $q = e/2$, $\mathbf{P} = (\mathbf{p}_1 - \mathbf{p}_2)/2$ and its coordinate $\mathbf{r} = \mathbf{r}_1 - \mathbf{r}_2$.

Notice that the effects of the spin and an applied uniform magnetic field can also be taken into account by simply replacing ω_0 with the effective frequency $\Omega = (\omega_0^2 + \omega_c^2/4)^{1/2}$ in the Hamiltonian, where $\omega_c = eB/m^*c$ is the cyclotron frequency, and adding the spin energy term $E_s = g^* \mu_B B S_z$ with $S_z = [1 - (-1)^m]/2$ to the total energy of the QD spectra. The relative Hamiltonian [Eq. (2)] can be written as

$$H_r = -\frac{\hbar^2}{2\mu} \left[\frac{1}{r} \frac{\partial}{\partial r} \left(r \frac{\partial}{\partial r} \right) + \frac{1}{r^2} \frac{\partial^2}{\partial \varphi^2} \right] + \frac{1}{2} \mu \omega_0^2 r^2 + \frac{e^2}{\epsilon r}. \quad (3)$$

By making the substitution

$$\phi(r) = r^{-1/2} \chi(r) e^{im\phi}$$

we obtain

$$\frac{d^2 \chi(r)}{dr^2} + \left(2\mu E/\hbar^2 - \frac{m^2 - \frac{1}{4}}{r^2} - \mu^2 \omega_0^2 r^2/\hbar^2 - \frac{2\mu e^2}{\hbar^2 \epsilon} \frac{1}{r} \right) \chi(r) = 0, \quad (4)$$

where $m=0, \pm 1, \pm 2 \dots$ is the azimuthal quantum number.

The eigenenergies for the center-of-mass motion can be exactly obtained as

$$E_{\text{cm}} = (2N_{\text{cm}} + |M_{\text{cm}}| + 1) \omega_0,$$

$$N_{\text{cm}} = 0, 1, 2, \dots, \quad M_{\text{cm}} = 0, \pm 1, \pm 2, \dots \quad (5)$$

The problem is reduced to solving the Hamiltonian of the relative motion, Eq. (2). By making the substitution $r = \sqrt{2}l_0x$, we write Eq. (2) as

$$\frac{d^2\chi(x)}{dx^2} + \left(\varepsilon - x^2 - \frac{\lambda}{x} - \frac{m^2 - \frac{1}{4}}{x^2} \right) \chi(x) = 0 \quad (6)$$

with

$$\varepsilon = E/(\hbar\omega_0)/2 \quad \text{and} \quad \lambda = \sqrt{2}l_0/a^*, \quad (7)$$

where λ is a tuning parameter and it measures the ratio of the Coulomb interaction to the harmonic confinement,

$$\lambda = \frac{\sqrt{2}l_0}{a^*} = 2\sqrt{R^*/\hbar\omega_0} \quad (8)$$

with an effective Bohr radius $a^* = \hbar^2\varepsilon/m^*e^2$.

The parameter $\lambda = \sqrt{2}l_0/a^*$ can be adjusted experimentally by varying the magnetic field strength B through the cyclotron frequency $\omega_c = eB/m^*c$. The change in ω_c results in a change of both the effective frequency $\Omega = (\omega_0^2 + \omega_c^2/4)^{1/2}$ and the effective characteristic length $l = (\hbar/m^*\Omega)^{1/2}$. In this case, both energies, the single-electron magnetoconfinement energy $E_q = (2n + |m| + 1)\Omega + m\omega_c/2$ and the many-body electron-electron interaction energy $E_c \sim e^2/\varepsilon l$, will change also.

Since Eq. (6), representing the problem of relative motion confined in a harmonic potential coupled with a Coulomb potential $V(x) = x^2 + \lambda/x$, cannot be solved exactly by any analytical methods, it is clear that we are going to resort to approximation methods.

III. CALCULATION METHOD

The shifted $1/N$ expansion method, N being the spatial dimension, is a pseudoperturbative technique in the sense that it proposes a perturbation parameter that is not related to the coupling constant.²⁷⁻³⁰

The method starts by writing the radial Schrödinger equation, for an arbitrary cylindrical symmetric potential, in N -dimensional space, as

$$\left[-\frac{d^2}{dr^2} + \frac{\bar{k}^2[1 - (1-a)/\bar{k}][1 - (3-a)/\bar{k}]}{4r^2} + \frac{V(r)}{Q} \right] \psi(r) = \varepsilon_{n_r, m} \psi(r), \quad (9)$$

where

$$V(r) = r^2 + \frac{\lambda}{r} \quad (10)$$

and $\bar{k} = N + 2m - a$, a is a shift parameter, and Q is a scaling constant to be determined. The shifted $1/N$ expansion

method consists of solving Eq. (9) in terms of the expansion parameter $1/\bar{k}$. It is convenient to shift the origin to r_0 by the definition

$$y = \bar{k}^{1/2}(r - r_0)/r_0 \quad (11)$$

and to expand Eq. (9) about $y=0$ in powers of y . Comparing the coefficients of powers of y in the series with the corresponding ones of the same order in the Schrödinger equation for a one-dimensional anharmonic oscillator, we determine the anharmonic oscillator frequency, the energy eigenvalue, the scaling constant, and the shift parameter in terms of \bar{k} , r_0 and the potential derivatives. The anharmonic frequency parameter is

$$\varpi = \left[3 + \frac{r_0 V''(r_0)}{V'(r_0)} \right]^{1/2} \quad (12)$$

the energy eigenvalues in powers of $1/\bar{k}$ (up to third order) read

$$\varepsilon_{n_r, m} = \frac{\lambda}{r_0} + r_0^2 + \frac{\bar{k}^2}{4r_0^2} + \frac{1}{r_0^2} \left[\frac{(1-a)(3-a)}{4} + \alpha_1 \right] + \frac{\alpha_2}{\bar{k}r_0^2}, \quad (13)$$

$$a = 2 - (2n_r + 1)\bar{\omega}, \quad (14)$$

$$\sqrt{2r_0^3 V'(r_0)} = 2 + 2m - a = Q^{1/2}, \quad (15)$$

where α_1 and α_2 parameters are expressed in terms of Q , $\bar{\omega}$, and n_r , and given in the Appendix. The roots r_0 (for particular quantum state and confining frequency) can be determined through Eqs. (14) and (15), and thus the task of computing the energy from Eq. (13) is relatively easy, n_r is the radial quantum number related to the principle (n) and magnetic (m) quantum number by the relation $n_r = n - |m| - 1$.

IV. RESULTS AND CONCLUSIONS

Our calculated results for QD's of two interacting electrons are presented in Figs. 1 and 2 and Tables I and II. We have considered QD's made of GaAs/Al_{1-x}Ga_xAs, with electron effective mass $m^* = 0.067m_0$ and dielectric constant 12.5. Table I compares the energy spectra of two independent ($\lambda=0$) and interacting ($\lambda=1$ and 10). The comparison between both cases clearly shows that the energy levels are enhanced by including the electron-electron ($e-e$) interaction Coulomb energy. For example, the energy of the quantum-dot state $|0,2\rangle$ increases significantly from 6 for $\lambda=0$ to 6.6536 and 11.7860 for $\lambda=1$ and 10, respectively. Thus the $e-e$ interaction term is very significant and its effects on the QD spectra manifest themselves in two ways: it removes the level degeneracy of the quantum-dot states and it also leads to the crossing between these QD levels. Both effects can be attributed to the new dependence of the Coulomb interaction energy on the quantum number (m), as we are going to show, and to the ratio of Coulomb to harmonic confinement energies λ .

These level crossings are the salient features of the QD spectra, which has been studied and analyzed to a great extent. In this discussion we shall work along this direction

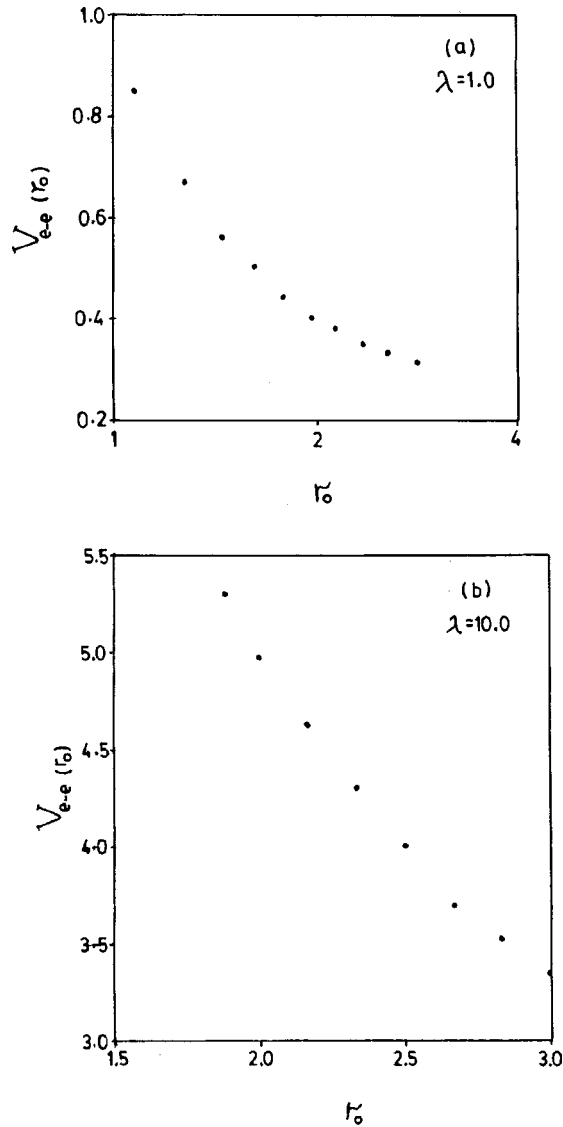


FIG. 1. The Coulomb interaction energy λ/r_0 as a function of roots r_0 corresponding to the quantum states $|0, m\rangle, m=0, +1, +2, \dots, +10$ for (a) $\lambda=1$ and (b) $\lambda=10$.

using the shifted $1/N$ expansion method. To explain both features, particular attention is paid to the dominant term: $V(r_0) = \lambda/r_0 + r_0^2$. This term contributes $\sim 50\%$ to the total energy of the quantum dot state. The energy of any quantum-dot state with different quantum numbers $|n_f, m\rangle$ and various λ can be computed using the energy series expression given in Eq. (13). This effective potential term, namely, $V(r_0) = \lambda/r_0 + r_0^2$, represents clearly a Coulomb and harmonic oscillator potentials. For a purely hydrogen atom the energy expectation value of the Coulomb potential is independent of the quantum number m . This is different from the expectation value of parabolic potential energy that shows a clear dependence on m . Now the effective two-electron Hamiltonian theory includes two potentials, the harmonic oscillator and the Coulomb potentials, which are in competition with each other. This is equivalent to saying that a harmonic oscillator force tries to push the electron to the center of the quantum dot while a Coulomb force tries to repel the electron towards the edge of the QD. The potential competition changes the dependence of the Coulomb $e-e$ interaction en-

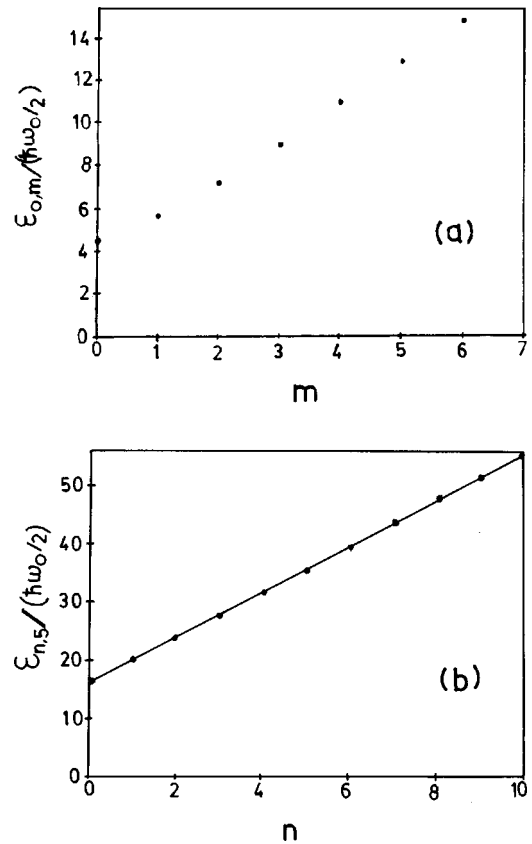


FIG. 2. The eigenenergies of the quantum dot spectra produced by $1/N$ expansion method (●●●) compared with the results of exact method (—) given in Ref. 21 for (a) $n=0, \lambda=2$ and (b) $m=5, \lambda=10$.

ergy on the quantum number m . This present behavior for the Coulomb potential energy receives detailed analysis in our study.

To investigate the dependence relation of the Coulomb term $\sim 1/r_0$ on m and λ through our method, we have calculated, first, the harmonic frequency $\bar{\omega}$ using Eq. (12) and, second, obtained the shifted parameter a through Eq. (14). Substituting both quantities in Eq. (15), we give the relation between the r_0, m , and λ variables,

$$[2(r_0^4 - \lambda r_0)]^{1/2} = 2|m| + \left[3 + \frac{2(r_0^3 - \lambda)}{(2r_0^4 - \lambda r_0)} \right]^{1/2}. \quad (16)$$

It is clear that finding the roots r_0 through Eq. (16) analytically in terms of m and λ is not attainable. Thus, we seek numerical solution and produce the roots r_0 for different m states and λ values as given in Fig. 1. We observe that the roots r_0 , for fixed λ , increase as m increases and thus the Coulomb energy $\sim 1/r_0$ tends to decrease. On the other hand, the confinement energy $\sim r_0^2$ is enhanced by increasing the quantum number m . These behaviors for Coulomb and confining potential terms are in agreement with the results of Maksym's and Chakraborty's work.¹² In Ref. 12, they found that the Coulomb energy (calculated and also shown in Fig. 2 for three interacting electrons) decreases as the total quantum number (J) increases, while the confining energy (single energy) increases as J increases also. The reduction in the electron-electron interaction energy, as λ/r_0 , does not con-

TABLE I. The energies of two interacting electrons in a quantum dot calculated by exact (Ref. 21) and $1/N$ expansion methods for $\lambda=1$ and 10. Energies are expressed in units of $\hbar\omega_0/2$.

$\lambda=0$		$\lambda=1$		$\lambda=10$			
$ n, m\rangle$	$\varepsilon_{n,m}$	$ n, m\rangle$	Exact	$1/N$	$ n, m\rangle$	Exact	$1/N$
$ 0, 0\rangle$	2	$ 0, 0\rangle$	3.4952	3.4234	$ 0, 0\rangle$	10.4816	10.4398
$ 0, 1\rangle$	4	$ 0, 1\rangle$	4.8553	4.8524	$ 0, 1\rangle$	10.8495	10.8341
$ 0, 2\rangle, 1, 0\rangle$	6	$ 0, 2\rangle$	6.6538	6.6535	$ 0, 2\rangle$	11.7903	11.7860
		$ 1, 0\rangle$	7.2340	7.2339	$ 0, 3\rangle$	13.0720	13.0717
$ 0, 3\rangle, 1, 1\rangle$	8	$ 0, 3\rangle$	8.5485	8.5484	$ 1, 0\rangle$	14.0379	14.0380
		$ 1, 1\rangle$	8.7594	8.7197	$ 1, 1\rangle$	14.4622	14.4621
$ 0, 4\rangle, 1, 2\rangle, 2, 0\rangle$	10	$ 0, 4\rangle$	10.4814	10.4814	$ 0, 4\rangle$	14.5546	14.5544
		$ 1, 2\rangle$	10.6024	10.6023	$ 1, 2\rangle$	15.4916	15.4915
		$ 2, 0\rangle$	11.0848	11.0848	$ 0, 5\rangle$	16.1628	16.1629
$ 0, 5\rangle, 1, 3\rangle, 2, 1\rangle$	12	$ 0, 5\rangle$	12.4340	12.4340	$ 1, 3\rangle$	16.8431	16.8431
		$ 1, 3\rangle$	12.5154	12.5153	$ 2, 0\rangle$	17.6671	17.6670
		$ 2, 1\rangle$	12.6961	12.6962	$ 0, 6\rangle$	17.6671	17.8541

sume completely the enhancement in the confinement energy as r_0^2 . This net competition energy between the Coulomb and confinement energies, which actually both constitute the dominant term $E^{(0)} = \lambda/r_0 + r_0^2$ in the energy series, removes the degeneracy of the quantum dot levels and also leads to the level crossings. For example, the states $|4\rangle$, $|1,2\rangle$, and $|2,0\rangle$, which are degenerate for independent ($\lambda=0$) with eigenenergy 10, are now split into three states with different energies 10.4814, 10.6023, and 10.0848, respectively, for the interacting case $\lambda=1$. The electron-electron interaction in

TABLE II. The energies of the quantum dot spectra calculated by $1/N$ expansion method for (a) $n=0$, $\lambda=2$ and (b) $m=5$, $\lambda=10$.

(a)	
m	$\varepsilon_{0,m}$
0	4.5421
1	5.6500
2	7.2865
3	9.0862
4	10.9564
5	12.8638
6	14.7936
7	16.7380
(b)	
n	$\varepsilon_{n,5}$
0	16.1629
1	20.0086
2	23.8586
3	27.7146
4	31.5795
5	35.4545
6	39.3390
7	43.2324
8	47.1347
9	51.0437
10	54.9601

this way removes the level degeneracy of the quantum dot spectra. In addition to this degeneracy lifting the electron-electron interaction energy changes the ordering of the quantum dot levels from $|0,0\rangle, |0,1\rangle, |0,2\rangle, |1,0\rangle, |0,3\rangle, |1,1\rangle, |0,4\rangle, |1,2\rangle, |2,0\rangle, |0,5\rangle, |1,3\rangle, |2,1\rangle$ for $\lambda=0$ to $|0,0\rangle, |0,1\rangle, |0,2\rangle, |0,3\rangle, |1,0\rangle, |1,1\rangle, |0,4\rangle, |1,2\rangle, |0,5\rangle, |1,3\rangle, |2,0\rangle, |0,6\rangle$ for $\lambda=10$. Particularly, the states $|1,0\rangle, |0,3\rangle$ for $\lambda=1$ change their order to $|0,3\rangle, |1,0\rangle$, for $\lambda=10$ and the level crossing occurs. The same thing happens for $|1,2\rangle, |2,0\rangle, |0,5\rangle, |1,3\rangle$, which changes to $|1,2\rangle, |0,5\rangle, |1,3\rangle, |2,0\rangle$. For finite large values of λ , the electron-electron interaction energy becomes more pronounced and the energy of the states with small m values, thus small r_0 and large λ/r_0 , from lower energy levels, significantly enhances and catches the states with large m values. This means a large r_0 and small λ/r_0 , from the higher-energy level. Our observation here agrees with Ref. 21. In this way the dependence of Coulomb energy on m and λ through $r_0 V_{e-e}(r_0, m, \lambda)$, explains the energy level crossings and the removal of the level degeneracy. As we mentioned earlier, these transitions in the angular momentum (m) and spin (s) of the ground state for the interacting electrons confined in the quantum dot appear as kinks in the electron addition energy spectra. Indeed these transitions have been predicted theoretically¹³ and also confirmed experimentally^{6,7,11} by different groups using quantum dots made from GaAs/Al_{1-x}Ga_xAs.

In addition to this qualitative explanation of the spectral properties of the quantum dot, we have tested the accuracy of the shifted $1/N$ expansion method against different numerical methods. In Figs. 2(a) and 2(b) and Table II, we have compared the energies, for different quantum states and various values of λ , computed by $1/N$ expansion method against the recently published results produced by Wontzel-Kramers-Brillouin (-Jeffreys) W.K.B.-double-parabola and exact numerical methods. The comparison clearly shows that the $1/N$ expansion method gives very accurate results compared with WKB and exact numerical methods. Almost perfect results are obtained for quantum-dot states with large quantum numbers, namely, n_r and m . Since large values of n_r and m mean that $\bar{k} = 2N + m - a$ is also large, the energy series expression

given in Eq. (13) converges very rapidly in terms of $1/\bar{k}$ expansion. For example, the energies of the state $|0,0\rangle$ calculated by $1/N$ and exact methods, respectively, are 3.4234 and 3.4952 for $\lambda = 1$ and 10.4398 and 10.4816 for $\lambda = 10$. On the other hand, the energies of the state $|0,5\rangle$ calculated with both methods, 12.4340 for $\lambda = 1$ and 16.8431, are exactly the same for the state $|1,3\rangle$ calculated at $\lambda = 10$.

In conclusion, we have studied the spectral properties of two interacting electrons in a quantum dot using the $1/N$ expansion method. With the dominant simple energy term $V(r_0) = \lambda/r_0 + r_0^2$, we are able to explain the level crossings

and the removal of the degeneracy as two interesting features, which are theoretically predicted and also experimentally confirmed in the spectra of the quantum dot. In addition to this explanation, the shifted $1/N$ expansion technique gives very accurate numerical results compared with WKB and exact methods.

APPENDIX

The parameters α_1 and α_2 appeared in Eq. (13) and are given as follows:

$$\alpha_1 = [(1 + 2n_r)e_2 + 3(1 + 2n_r + 2n_r^2)e_4] - \varpi^{-1}[e_1^2 + 6(1 + 2n_r)e_1e_3 + (11 + 30n_r + 30n_r^2)e_3^2],$$

$$\alpha_2 = (1 + 2n_r)d_2 + 3(1 + 2n_r + 2n_r^2)d_4 + 5(3 + 8n_r + 6n_r^2 + 4n_r^3)d_6 - \varpi^{-1}[(1 + 2n_r)e_2^2 + 12(1 + 2n_r + 2n_r^2)e_2e_4 + 2e_1d_1$$

$$+ 2(21 + 59n_r + 51n_r^2 + 34n_r^3)e_4^2 + 6(1 + 2n_r)e_1d_3 + 30(1 + 2n_r + 2n_r^2)e_1d_5 + 6(1 + 2n_r)e_3d_1 + 2(11 + 30n_r + 30n_r^2)e_3d_3$$

$$+ 10(13 + 40n_r + 42n_r^2 + 28n_r^3)e_3d_5] + \varpi^{-2}[4e_1^2e_2 + 36(1 + 2n_r)e_1e_2e_3 + 8(11 + 30n_r + 30n_r^2)e_2e_3^2 + 24(1 + n_r)e_1^2e_4$$

$$+ 8(31 + 78n_r + 78n_r^2)e_1e_3e_4 + 12(57 + 189n_r + 225n_r^2 + 150n_r^3)e_3^2e_4] - \varpi^{-3}[8e_1^3 + 108(1 + 2n_r)e_1^2e_3^2$$

$$+ 48(11 + 30n_r + 30n_r^2)e_1e_3^2 + 30(31 + 109n_r + 141n_r^2 + 94n_r^3)e_3^4]$$

with $e_j = \varepsilon_j/\varpi^{j/2}$ and $d_i = \delta_i/\varpi^{i/2}$, where $j = 1, 2, 3, 4$, $i = 1, 2, 3, 4, 5, 6$.

The definition of ε_j and δ_i quantities are

$$\varepsilon_1 = (2 - a), \quad \varepsilon_2 = -3(2 - a)/2,$$

$$\varepsilon_3 = -1 + r_0^5 V^{(3)}(r_0)/6Q, \quad \varepsilon_4 = \frac{5}{4} + \frac{r_0^6 V^{(4)}(r_0)}{24Q},$$

$$\delta_1 = -(1 - a)(3 - a)/2, \quad \delta_2 = 3(1 - a)(3 - a)/4,$$

$$\delta_3 = 2(2 - a), \quad \delta_4 = -5(2 - a)/2,$$

$$\delta_5 = -\frac{3}{2} + r_0^7 V^{(5)}(r_0)/120Q, \quad \delta_6 = \frac{7}{4} + r_0^8 V^{(6)}(r_0)/720Q.$$

-
- ¹H. Drexler, D. Leonard, W. Hansen, J. P. Kotthaus, and P. M. Petroff, Phys. Rev. Lett. **73**, 2252 (1994).
²C. Sikorski and U. Merkt, Phys. Rev. Lett. **62**, 2164 (1989).
³T. Demel, D. Heitmann, P. Grambow, and K. Ploog, Phys. Rev. Lett. **64**, 788 (1990).
⁴A. Lorke, J. P. Kotthaus, and K. Ploog, Phys. Rev. Lett. **64**, 2259 (1990).
⁵A. Wixforth *et al.*, Semicond. Sci. Technol. **9**, 215 (1994).
⁶R. C. Ashoori, H. L. Stormer, J. S. Weiner, L. N. Pfeiffer, K. W. Baldwin, and K. W. West, Phys. Rev. Lett. **71**, 613 (1993).
⁷R. C. Ashoori, Nature (London) **379**, 413 (1996).
⁸S. R. Eric Yang, A. H. MacDonald, and M. D. Johnson, Phys. Rev. Lett. **71**, 3194 (1993).
⁹S. Tarucha, D. G. Austing, T. Honda, R. J. Vander, and L. D. Kouwenhoven, Phys. Rev. Lett. **77**, 3613 (1996).
¹⁰T. H. Oosterkamp, J. W. Janssen, L. P. Kouwenhoven, D. G. Austing, T. Honda, and S. Tarucha, Phys. Rev. Lett. **82**, 2931 (1999).
¹¹L. P. Kouwenhoven, T. H. Oosterkamp, M. W. S. Danoesarto, M. Eto, D. G. Austing, T. Honda, and S. Tarucha, Science **278**, 788 (1997).
¹²P. A. Maksym and T. T. Chakraborty, Phys. Rev. Lett. **65**, 108 (1990).
¹³M. Wagner, U. Merkt, and A. V. Chaplik, Phys. Rev. B **45**, 1951 (1992).
¹⁴D. Pfannkuche and R. R. Gerhardts, Physica B **189**, 6 (1993).
¹⁵J. J. S. De Groote, J. E. M. Honos, and A. V. Chaplik, Phys. Rev. B **46**, 12 773 (1992).
¹⁶U. Merkt, J. Huser, and M. Wagner, Phys. Rev. B **43**, 7320 (1991).
¹⁷D. Pfannkuche and R. R. Gerhardts, Phys. Rev. B **44**, 13 132 (1991).
¹⁸K. D. Zhu and S. W. Gu, Phys. Lett. A **172**, 296 (1993).
¹⁹N. F. Jhonson and M. C. Payne, Phys. Rev. Lett. **67**, 1157 (1991).
²⁰S. Klama and E. G. Mishchenko, J. Phys.: Condens. Matter **10**, 3411 (1998).
²¹R. M. G. Garcia-Castelan, W. S. Choe, and Y. C. Lee, Phys. Rev. B **57**, 9792 (1998).

- ²²E. Anisimovas and A. Matulis, *J. Phys.: Condens. Matter* **10**, 601 (1998).
- ²³A. Matulis and P. M. Peeters, *J. Phys.: Condens. Matter* **6**, 775 (1994).
- ²⁴Y. M. Blanter, N. E. Kaputkina, and Y. E. Lozovik, *Phys. Scr.* **54**, 539 (1996).
- ²⁵F. M. Peeters and V. A. Schweigert, *Phys. Rev. B* **53**, 1468 (1996).
- ²⁶J. H. Oh, K. J. Chang, G. Ihm, and S. J. Lee, *Phys. Rev. B* **53**, 13 264 (1996).
- ²⁷T. Imbo, A. Pagnamento, and U. Sukhatme, *Phys. Rev. D* **29**, 8763 (1984).
- ²⁸T. Imbo and U. Sukhatme, *Phys. Rev. D* **28**, 418 (1983); **31**, 2655 (1985).
- ²⁹R. Dutt, U. Mukherji, and Y. P. Varshni, *J. Phys. B* **19**, 3411 (1986).
- ³⁰M. El-Said, *Semicond. Sci. Technol.* **10**, 1310 (1995).